Critical behavior at transitions from uniaxial to biaxial phases in a smectic liquid-crystal mixture

Y. Sasaki and K. Ema*
Department of Physics, Tokyo Institute of Technology, 2-12-1 O-okayama, Meguro, Tokyo 152-8551, Japan

K. V. Le and H. Takezoe
Department of Organic and Polymeric Materials, Tokyo Institute of Technology, 2-12-1 O-okayama, Meguro, Tokyo 152-8552, Japan

S. Dhara
School of Physics, University of Hyderabad, Hyderabad 500046, India

B. K. Sadashiva
Raman Research Institute, C. V. Raman Avenue, Bangalore 560080, India

(Received 17 March 2010; published 29 July 2010)

We report results of calorimetric and optical investigations of binary mixtures of rodlike and bent-shaped molecules. We find that the observed critical heat anomaly associated with the smectic-A_2 to biaxial smectic-A_{2b} transition is well described with a Fisher-renormalized form of the usual scaling expression. The effect of renormalization is large in this system in part because of the moderately steep slope of the phase boundary ($dT_c/dX \sim 100$ K, where X is the mole fraction of the bent-core molecules) and in part because of the proximity to the tricritical point. The magnitude of heat anomaly at the smectic-A_2–smectic-A_{2b} transition showed a drastic decrease as X becomes smaller. Moreover, the nematic–smectic-A_2 transitions investigated turned out to be always first order and the transition enthalpy showed only weak dependence on the concentration X. The results imply that the energy fluctuations around the smectic-A_2–smectic-A_{2b} transition are very sensitive to the underlying ordering of the smectic-A_2 background.

DOI: 10.1103/PhysRevE.82.011709 PACS number(s): 64.70.M−, 64.60.F−, 65.40.Ba

I. INTRODUCTION

Liquid-crystal mixtures formed from bent-shaped molecules and rodlike molecules have been extensively studied in the last two decades. Remarkable numbers of new phases have been found (see, for instance, Refs. [1–3]). One of the recent significant researches [1] reported the discovery of an orientational transition of bent-shaped molecules in a background medium of smectic (Sm) liquid crystal formed from rodlike molecules. The structures of bent-shaped molecule 1,3-phenylene-bis[4-(3-methylbenzoyloxy)]-4′-*n*-dodecylbiphenyl-4′-carboxylate (BC12) and rodlike molecule 4-biphenylyl-4″-*n*-undecyloxybenzoate (BO11), used in their work, are shown in Fig. 1. When the mole fraction of BC12 molecules (denoted as X) is small, the phase sequence of mixtures has been reported as I(isotropic)–N(nematic)–Sm(smectic)-A_2–SmA_{2b}–Cr(crystal). Here, the SmA_{2b} phase has been found as a novel smectic phase with biaxiality induced by an orientational ordering of the minor amounts of bent-core molecules in the mixture. Such an ordering phenomenon of bent-shaped molecules embedded in the SmA_2 background is unusual and, therefore, of special interest. Although the work by Pratibha *et al.* [1,2] included extensive studies of the ordering in the system by optical, x-ray, and other methods, thermal properties were not studied in detail except some differential calorimetric analyses. In particular, based on the reasons described below, this mixture system deserves attention from two points of view: (A) a very steep X dependence of the SmA_2-SmA_{2b} transition temperature and (B) the existence of the N-SmA_2 transition for a substantially wide X range.

According to the phase diagram [1], the SmA_2-SmA_{2b} phase boundary has a very steep slope of $dT_c/dX \sim 100$ K. Generally, such cases are remarkable because we can observe the so-called Fisher renormalization [4]. Usually, measurements are performed as a function of $t_X \equiv T/T_c(X) - 1$ along a path with constant X. Here, $T_c(X)$ is the measured transition temperature. Keeping the chemical potential difference ϕ constant in the mixture can significantly influence the underlying critical behavior of the system considered as a thermodynamic constraint. It is well known that C_{pX} values measured along a constant composition path should exhibit a different behavior from $C_{p\phi}$, the heat capacity at a constant chemical potential difference. Obtaining true critical behavior requires the measurement of $C_{p\phi}$ as a function of $t_\phi \equiv T/T_c(\phi) - 1$. As a consequence of this, as Fisher [4]

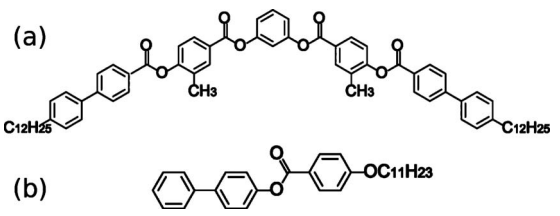

FIG. 1. Structures of (a) bent-core molecule (BC12) 1,3-phenylene-bis[4-(3-methylbenzoyloxy)]-4′-*n*-dodecylbiphenyl-4′-carboxylate and (b) rodlike molecule (BO11) 4-biphenylyl-4″-*n*-undecyloxybenzoate.

*Author to whom correspondence should be addressed. kema@phys.titech.ac.jp

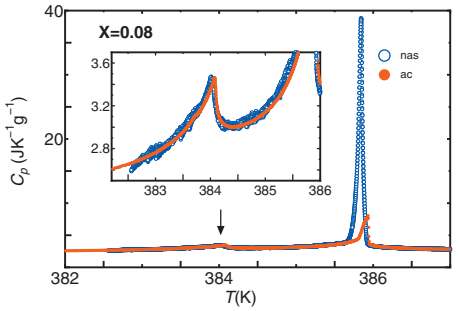

FIG. 2. (Color) Heat capacity near the N-SmA_2 and the SmA_2-SmA_{2b} transitions at $X=0.08$. Here, X is the mole fraction of BC12 molecules.

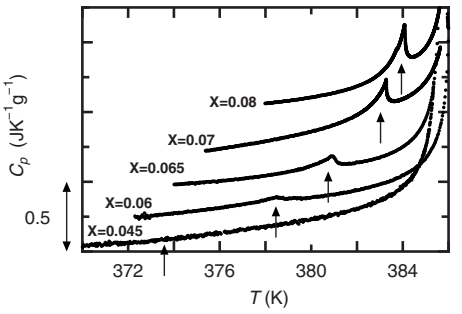

FIG. 3. Heat-capacity data obtained for five mixture ratios. The arrows indicate the position of the SmA_2-SmA_{2b} transition.

pointed out, the critical exponent has been renormalized to give $\alpha_X=-\alpha/(1-\alpha)$. Since the critical exponent α characterizes the leading singularity of the heat anomaly, this corresponds to a crossover from divergent power-law behavior ($\alpha>0$) to finite cusplike renormalized behavior ($\alpha_X<0$) in C_{pX}. In the heat-capacity measurements, this phenomenon has been observed, for example, in ^{3}He-^{4}He mixtures [5], several rodlike liquid-crystal mixtures [6–8], and liquid mixtures [9]. Furthermore, the extent of such a renormalization significantly depends on the values of α and $(T_c^{-1}dT_c/dX)$ [9,10]. In particular, when $\alpha=0.5$, the magnitude of renormalized exponents is "doubled" as $\alpha_X=-1$, giving rise to a drastic change.

Another issue of special interest here is the behavior of the N-SmA transition. So far, a series of N-SmA transitions has been studied through theoretical and experimental approaches, particularly relating to the so-called McMillan ratio $T_{\mathrm{NA}}/T_{\mathrm{IN}}$ [11,12], with T_{NA} and T_{IN} being the N-SmA transition and the I-N transition temperatures. The coupling between the smectic density-wave amplitude ψ and the magnitude S of the nematic order parameter causes a crossover toward a tricritical point and eventually leads to a first-order transition as $T_{\mathrm{NA}}/T_{\mathrm{IN}}\rightarrow 1$. According to McMillan [13], the tricritical point takes place at the value of 0.87, although this value is not universal and experimental data report slightly higher values compared with the expectation [14]. Some first-order N-SmA transitions were found [15,16] when the nematic range becomes very narrow, i.e., $T_{\mathrm{NA}}/T_{\mathrm{IN}}>0.99$. It has been noticed that the tricriticality occurs at different McMillan ratios depending on different types of SmA phases [7,17], although experimental studies are quite limited with regard to SmA_2 phase.

In this paper, we report extensive calorimetric and optical investigations on pure BO11 and mixtures of BO11 and BC12 with $X=0.045-0.10$. The obtained data indicate the existence of a tricritical point along the SmA_2-SmA_{2b} phase boundary. The heat anomaly associated with the SmA_2-SmA_{2b} transition showed cusplike behavior near the tricritical point and can be well understood as the appearance of Fisher-renormalized tricritical behavior in the vicinity of T_c. It was also found that the magnitude of the heat anomaly drastically diminishes with decrease in X. On the other hand, the N-SmA_2 transition was found to be first order for pure BO11 as well as for mixtures, while the transition enthalpy showed only weak dependence on X. These results imply that the energy fluctuations around the smectic-A_2–smectic-A_{2b} transition are very sensitive to the underlying ordering of the smectic-A_2 background.

II. METHODS AND RESULTS

The calorimetric investigation has been performed in a low-frequency ac mode [18] as well as a nonadiabatic scanning (nas) mode [19]. Nas mode allows one to measure the enthalpy as a function of the temperature at first-order transitions, while ac mode can determine precise pretransitional changes in heat anomalies. Samples of about 7 mg were placed in hermetically sealed gold cells. Temperature scan rate was about 0.03 K/h near the transition region.

Figure 2 shows the temperature dependence of the heat capacity at $X=0.08$. A large anomaly is evident at a temperature of about 385.8 K, which corresponds to the N-SmA_2 transition. The heat-capacity anomaly obtained by nas mode is much larger than that obtained by ac mode. Another small peak around 384.1 K corresponds to the SmA_2-SmA_{2b} transition where ac and nas modes gave essentially the same result, in contrast to the N-SmA_2 transition. This indicates that the transition is second order with no measurable latent heat. In addition, the heat anomaly at the SmA_2-SmA_{2b} transition exhibits cusplike behavior. For $0.045\leqq X\leqq 0.08$, heat-capacity data showed almost the same trend as described for $X=0.08$. However, the magnitude of the SmA_2-SmA_{2b} heat anomaly decreased sharply with the decrease in X as shown in Fig. 3 while the transition enthalpy associated with N-SmA_2 did not show strong dependence on concentration. For example, the N-SmA_2 transition enthalpies measured at

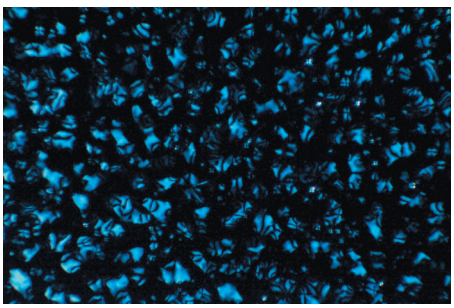

FIG. 4. (Color) Coexistence of SmA_2 and SmA_{2b} phases in a homeotropically aligned cell for a sample with $X=0.09$.

$X=0.045$ and $X=0.08$ are ~2.2 and ~2.6 kJ/mol, respectively. Furthermore, the calorimetric measurement on pure BO11, which has a nematic range of 14.5 K, turned out to be also first order with the enthalpy of ~2.1 kJ/mol.

When $X=0.09$, the heat-capacity data at the SmA_2-SmA_{2b} transition measured by nas mode showed a slightly larger peak than the one by ac mode. The existence of latent heat seems plausible. However, since N-SmA_2 and SmA_2-SmA_{2b} transitions approach each other, they cannot be distinguished clearly. Optical measurement at the composition has been performed to obtain solid evidence. As shown in Fig. 4, a clear coexistence of the two phases has been observed in a homeotropically aligned cell (alignment layer: polyimide JALS-204 from JSR, Japan) where the black domain is SmA_2 and the bluish one is SmA_{2b}. Judging from calorimetric and optical investigations, the transition at $X=0.09$ is first order.

The phase diagram based on the above results is shown in Fig. 5. A tricritical point is located between $X=0.08$ and 0.09 on the moderately steep SmA_2-SmA_{2b} transition line $dT_c/dX \sim 100$ K. The overall appearance of the phase diagram is in good agreement with the original phase diagram [1], while somewhat small differences in transition temperatures have been noticed. This is probably because of the slow temperature scan rate in ac calorimetry as compared with commercial differential scanning calorimetric and optical measurements.

To estimate the excess heat capacity ΔC_{pX} accompanying the SmA_2-SmA_{2b} transition, the pretransitional background related to the N-SmA_2 transition has been determined and subtracted from the observed C_{pX} data. Then, the ΔC_{pX} data have been analyzed with the following renormalization-group expression in terms of the reduced temperature t_X including corrections to scaling [20,21]:

$$\Delta C_{pX} = A^{\pm}|t_X|^{-\alpha}(1 + D_1^{\pm}|t_X|^{\theta}) + B_c, \tag{1}$$

where $\pm$ indicates above and below T_c. Theoretically expected correction-to-scaling exponent θ values are approximately 0.5 for three-dimensional (3D) cases [22] and fixed to 0.5 in the present fittings. B_c is a constant term that arises from the critical background. In general, when one carries out critical exponent analysis, data points close to T_c should be excluded from the fit due to inhomogeneities of the mixture and/or instrumental errors associated with the finite size of the temperature oscillations ΔT_{ac}. The limit of the rounding region has been estimated according to the procedure described in [23] by examining χ_ν^2,

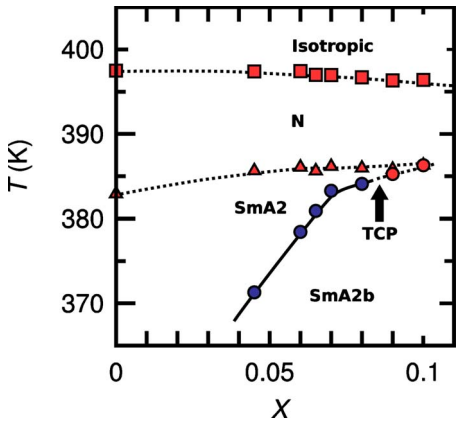

FIG. 5. (Color online) Phase diagram of BO11/BC12 binary mixtures. Solid and dashed lines show second- and first-order transitions, respectively. The temperature width of two-phase coexistence region at the first-order transitions is quite narrow in this scale, being on the order of 0.1 K, or at most 0.5 K, so that it is not shown here.

$$\chi_\nu^2 = \frac{1}{\nu}\sum_i^n \left(\frac{1}{\sigma_i^2}[\Delta C_{pi}^{\rm obs} - \Delta C_{pi}^{\rm fit}(T_i)]^2 \right), \tag{2}$$

where $\Delta C_{pi}^{\rm obs}$ and $\Delta C_{pi}^{\rm fit}$ denote the measured and calculated heat capacities, respectively. σ_i is a standard deviation of $\Delta C_{pi}^{\rm obs}$ and ν is the number of degrees of freedom.

Table I lists the result of the fits with Eq. (1) for $X=0.08$. Here, $|t|_{\rm max}$ is the maximum value of $|t_X|$ used in the fit. When the first correction-to-scaling terms ($D_1^{\pm}$ terms) are included, α values are clearly negative and sensitive to the data range shrinking. The amplitude ratio A^-/A^+ also depends significantly on $|t|_{\rm max}$. Moreover, the ratio D_1^-/D_1^+ is large negative values, violating the theoretical expectation $D_1^+ = D_1^-$ [24]. For comparison, imposing $D_1^{\pm}=0$ gives fits of poor quality, indicating that $D_1^{\pm}$ terms play an important role anyway. These results show that Eq. (1) does not describe the observed heat anomaly adequately. Since the slope of the SmA_2-SmA_{2b} transition temperatures is steep, the above features suggest the appearance of Fisher renormalization.

TABLE I. Results of fits to the heat-capacity data at $X=0.08$ using Eq. (1). The minimum reduced temperatures showing the rounding region for $T>T_c$ and $T<T_c$ are determined as $|t|_{\rm min}^+ = 2.60\times10^{-6}$ and $|t|_{\rm min}^- = 6.25\times10^{-5}$, respectively. The units are J K^{-1} g^{-1} for $A^{\pm}$ and B, and K for T_c. The parameters in brackets were held fixed at the shown value in the fits.

$\lvert t\rvert_{\rm max}$	α	T_c	A^+	A^-/A^+	D^+	D^-/D^+	B	χ_ν^2
0.0005	−0.252	384.099	−5.6276	0.2348	−9.31	−3.87	0.8041	1.24
0.0005	0.013	384.097	7.0174	1.0414	[0]	[1]	−7.6019	6.33
0.0010	−0.184	384.100	−3.4163	0.3413	−4.88	−4.89	0.8965	1.34
0.0010	0.088	384.096	0.5498	1.2752	[0]	[1]	−0.9259	20.4
0.0030	−0.074	384.099	−2.9143	0.7221	−1.46	−2.72	1.7531	4.35
0.0030	0.193	384.089	0.1272	1.4348	[0]	[1]	−0.3970	165

TABLE II. Results of fits to the heat-capacity data at $X=0.07$ using Eq. (3). The minimum reduced temperatures showing the rounding region for $T>T_c$ and $T<T_c$ are determined as $|t|^{+}_{\min}=2.61\times10^{-6}$ and $|t|^{-}_{\min}=7.83\times10^{-6}$, respectively. The units are J K^{-1} g^{-1} for $\bar{A}^{\pm}$ and $\bar{B}$, and K for T_c. The parameters in brackets were held fixed at the shown value in the fits.

$\lvert t\rvert_{\max}$	α_X	$\bar{B}$	T_c	$\bar{A}^{+}$	$\bar{A}^{-}/\bar{A}^{+}$	$\bar{D}^{+}$	$\bar{D}^{-}/\bar{D}^{+}$	χ^2_ν
0.0004	−0.804	0.4597	383.280	918.288	0.1084	2273.4	0.1127	2.59
0.0005	−0.779	0.4597	383.280	703.682	0.1036	1714.3	0.0791	2.42
0.0010	−0.628	0.4672	383.280	155.884	0.1247	326.48	0.0297	2.39
0.0030	−0.558	0.4876	383.280	85.338	0.1622	160.47	0.0579	2.39
0.0004	[−1]	0.4531	383.279	5880.95	0.0934	16097	0.1362	3.22
0.0005	[−1]	0.4504	383.279	5654.69	0.0854	15449	0.1039	3.30
0.0010	[−1]	0.4419	383.278	4257.58	0.0865	10993	0.0781	6.39
0.0030	[−1]	0.4316	383.274	2889.86	0.1062	7041.6	0.0838	11.2

Consequently, on the basis of the relationship between ΔC_{pX} and $\Delta C_{p\phi}$, we have attempted the use of the following expression [7]:

$$\Delta C_{pX} = \bar{B} - \frac{\bar{A}^{\pm}|t_X|^{-\alpha_X}}{1+\bar{D}^{\pm}|t_X|^{-\alpha_X}}, \tag{3}$$

where the parameters $\bar{A}$, $\bar{B}$, and $\bar{D}$ can be regarded as constant in the vicinity of T_c although they have slight temperature dependence. It should be noted that the $\bar{D}$ term is not a correction-to-scaling term, unlike the D_1 term in Eq. (1). Before analyzing the data, the rounding region has been determined again using Eq. (3) instead of Eq. (1). This process plays a particularly nontrivial role when nondivergent behavior is the intrinsic physical property. Since Fisher renormalization is the very asymptotic behavior near T_c, eliminating the data around T_c causes the loss of important information. Like our system under consideration, when the renormalized region is expected to appear only in the immediate vicinity of T_c, the effect is distinct. As a result of employing Eq. (3), the new temperature region omitted becomes narrower than that estimated by using Eq. (1). The rounding region determined is $-7.83\times10^{-6}<t_X<2.61\times10^{-6}$ for $X=0.07$ and $-4.17\times10^{-5}<t_X<5.21\times10^{-6}$ for $X=0.08$. If divergent behavior occurs, the rounding region should expand owing to the renormalized expression of Eq. (3). We believe this result reflects that the shape of the heat anomaly very close to T_c is cusplike rather than divergent. Tables II and III list the results of the fits with Eq. (3) at $X=0.07$ and 0.08, respectively. In both cases, effective α_X values approach the fully renormalized tricritical value of $\alpha_X=-1$ as $|t|_{\max}$ becomes small as shown in these tables. To verify this tendency, fits were also tried with α_X fixed at −1, and the results are included in Tables II and III. It is seen that these fits are statistically worse than those with free α_X values especially for wider data ranges. The χ^2_ν value becomes less for smaller $|t|_{\max}$ fits and approaches the value obtained for the free α_X fits. Such a behavior is just expected as the result of the crossover from divergent behavior far from T_c to a Fisher-renormalized cusp near T_c. Figure 6 shows the ΔC_p data and fitting curves for $X=0.07$. The data close T_c illustrated above in Fig. 6 shows clearly cusplike behavior. The dashed line in the figure, showing the result of the fit obtained for data range $|t|_{\max}=0.0004$, deviates considerably from the data far from T_c. This is also in accordance with the range dependence of α_X described above. Nevertheless, the obtained α_X is not closer

TABLE III. Results of fits to the heat-capacity data at $X=0.08$ using Eq. (3). The minimum reduced temperatures showing the rounding region for $T>T_c$ and $T<T_c$ are determined as $|t|^{+}_{\min}=5.21\times10^{-6}$ and $|t|^{-}_{\min}=4.17\times10^{-5}$, respectively. The units are J K^{-1} g^{-1} for $\bar{A}^{\pm}$ and $\bar{B}$, and K for T_c. The parameters in brackets were held fixed at the shown value in the fits.

$\lvert t\rvert_{\max}$	α_X	$\bar{B}$	T_c	$\bar{A}^{+}$	$\bar{A}^{-}/\bar{A}^{+}$	$\bar{D}^{+}$	$\bar{D}^{-}/\bar{D}^{+}$	χ^2_ν
0.0004	−0.965	0.6769	384.090	5904.60	0.0876	9880.1	0.0719	2.87
0.0005	−0.843	0.6866	384.091	1880.88	0.0983	2918.5	0.0552	3.01
0.0010	−0.646	0.7177	384.092	307.652	0.1337	402.81	0.0407	2.82
0.0030	−0.550	0.7681	384.092	140.303	0.1813	160.73	0.0819	3.82
0.0004	[−1]	0.6744	384.090	8083.04	0.0859	13733	0.0766	2.87
0.0005	[−1]	0.6729	384.089	7656.06	0.0889	12810	0.0776	3.44
0.0010	[−1]	0.6674	384.086	6148.38	0.1070	9780.2	0.0940	6.99
0.0030	[−1]	0.6448	384.078	3969.10	0.1394	6035.9	0.1138	16.5

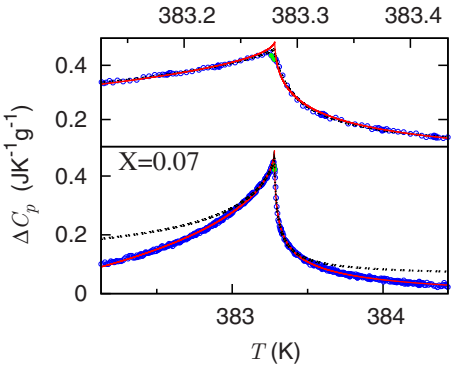

FIG. 6. (Color online) Excess heat-capacity ΔC_p data of the $X=0.07$ sample shown for two temperature ranges with $|t|_{\max}=0.0004$ (upper data set) and $|t|_{\max}=0.003$ (lower data set). Solid and dashed lines represent fits to the data with Eq. (3). The solid line is for $|t|_{\max}=0.003$, and the dashed line is for $|t|_{\max}=0.0004$.

to the fully renormalized exponent than that obtained for $X=0.08$.

We also note that, if we pay attention to numerical aspects without considering physical meanings, χ^2_ν values shown in Tables II and III with Eq. (3) are comparable with the result including $D_1^{\pm}$ in Table I. However, the violation of theoretical expectation $D_1^-/D_1^+=1$ mentioned above indicates that the fits with Eq. (1) and nonzero $D_1^{\pm}$ are artificial and therefore less reliable.

III. DISCUSSION

A. N-SmA_2 transition

The present investigation provides a rare example where the N-SmA_2 transition has been studied. The measurement revealed that N-SmA_2 phase transitions in this system are first order with large C_p peaks. Judging from the fact that the nematic range as well as the N-SmA_2 transition temperatures is essentially independent of X, it is expected that the nature of the first-order transitions does not arise from the effect of the mixing of bent-core molecules. This means that the SmA_2 structure plays a role of relatively stable background for BC12 molecules. The obtained nematic range of BO11 is about 15 K and larger than that of earlier reports of first-order N-SmA_d transitions [15,16]. The $T_{\mathrm{NA}}/T_{\mathrm{IN}}$ value of BO11 is 0.964 and, for example, almost the same as that observed in 4-n-octyloxy-4′-cyanobiphenyl (8OCB) exhibiting a second-order N-SmA_d transition with $\alpha\sim 0.2$ [14]. A second-order N-SmA_2 transition has also been reported for a compound with a large nematic range of 65 K with the accompanying heat anomaly being described well by the 3D-XY behavior [25]. Therefore, we can expect the existence of N-SmA_2 tricritical behavior as the nematic region grows as was expected in [25]. In particular, our data serve as a clear evidence that the $T_{\mathrm{NA}}/T_{\mathrm{IN}}$ value at a tricritical point is nonuniversal or that the dependence on $T_{\mathrm{NA}}/T_{\mathrm{IN}}$ values exhibited for $N-$SmA_2 transitions differs from other types of N-SmA transitions.

B. SmA_2-SmA_{2b} transition

It must be emphasized that the fully renormalized critical exponents are visible only close to T_c. In this sense, a crossover appears from the underlying nonrenormalized values to the fully renormalized ones. The temperature range where Fisher renormalization is visible experimentally is given by [10]

$$\tau=\left[A_0X(1-X)\left(\frac{1}{T_c}\frac{dT_c}{dX}\right)\right]^{1/\alpha}. \tag{4}$$

Here, A_0 is the amplitude of the nonrenormalized heat anomaly in units of R. For small critical exponent values like Ising critical behavior, the observation of Fisher renormalization is expected to be difficult. However, from an experimental point of view, Fisher renormalization has been observed over a wide range compared to the theory [7]. On the other hand, the effect becomes more pronounced in the case of the tricritical behavior. A suitable parameter for that case to characterize the dependence in Eq. (4) is $Z\equiv(T_c^{-1}dT_c/dX)^2$, where α is fixed at 0.5. Then Eq. (4) becomes $\tau=A_0^2X^2(1-X)^2Z^2$. A fully renormalized tricritical behavior over a substantial temperature range has been observed at several systems with Z ranging from 0.74 to 0.2 [7,8]. In our system considered, it turned out that $Z=0.067$. This value is small but accessible experimentally. In fact, if one assumes $A_0\sim 0.1$, this yields $\tau\sim 10^{-4}$, which does not seem to be an unrealistic estimation.

To check the validity of the analyses, both the critical exponent α and the universal amplitude ratio A^-/A^+ are important factors because they are highly correlated with each other. The results of the fits with Eq. (1) give an asymmetric and nonuniversal feature of heat anomaly. The possibility of the 3D-XY ($A^-/A^+\sim 0.97$ [26]) or the 3D-Ising ($A^-/A^+\sim 1.85$ [27]) behavior is ruled out. Tables II and III also show nonuniversal values. If we adopt the tricritical behavior, these features of A^-/A^+ ratios are not an issue of concern because tricritical A^-/A^+ ratios are not universal. Our result is also supported by the report in [1], where an exponent associated with the refractive indices has been estimated as $\beta\sim 0.67$. This large value can be explained by taking Fisher renormalization into account, because critical exponents should be doubled at a tricritical point.

Furthermore, it deserves attention that the magnitude of the heat anomaly diminishes drastically as X decreases. As mentioned in Sec. III A, the transition is caused essentially by BC12 molecules floating in the "sea" of SmA_2 structure formed from BO11 molecules. Therefore, the ΔC_p amplitude has a natural dependence proportional to X since the data are shown in the unit of mass of total mixture, although the observed decrease is obviously much faster. From the concept of the two-scale-factor universality [28,29], such a decrease in heat anomaly implies a rapid increase in the correlation length. With the hyperscaling relation $2-\alpha=d\nu$, it is expected that the specific heat amplitude A and the correlation volume satisfy the following relation in smectic phases:

$$A\xi_\parallel\xi_\perp^2=\text{const.} \tag{5}$$

If we assume that the correlation length grows simply geometrically in accordance with the distance between correlated bent-core molecules as X decreases, we obtain from Eq. (5) another multiplying factor proportional to X. This gives

rise to an X dependence being proportional to X^2 since we already have the above-mentioned factor that is proportional to X coming from the measuring unit. Nevertheless, the observed decrease is clearly still faster. The third and seemingly most effective factor for the C_p anomaly diminishing is the suppression of the energy fluctuation coming from the saturation of the underlying order parameter, as observed in the case of N-SmA transitions [30–33]. In those cases the width of the N phase is very sensitive to parameters such as the homolog number [30], mixture ratio [31,32], pressure [33], etc. As the underlying order for the present case, we can think of the extent of how well the BC12 molecules sit in the SmA_2 framework of BO11 molecules. Our data give the SmA_2 phase width being ~3 K for $X=0.07$ and ~14 K for $X=0.045$, differing by a factor of ~4.5. From Fig. 4 of Ref. [31], this amount of difference will yield the C_p anomaly magnitude differ by several tens of times. Although this estimation may be rather crude, the observed reduction in the C_p anomaly in our Fig. 3 seems to be explained. In any case, the drastic decrease in $A^{\pm}$ also implies that the renormalized region depends on the concentration. Therefore, the heat anomaly of $X=0.07$ should have a narrower renormalized region than that of $X=0.08$, which leads to the result that the effective critical exponent value α_X of $X=0.08$ is closer to $\alpha_X=-1$.

In conclusion, high-resolution calorimetric studies established a crossover phenomenon from underlying behavior far away from T_c to Fisher-renormalized tricritical behavior near T_c. Moreover, the measurements of the transitional enthalpy revealed a clear evidence of an example of first-order N-SmA_2 transition with a wide nematic temperature range. The results support the idea that the SmA_2 structure serves as a relatively stable background for the bent-shaped molecules. In addition, the dramatic reduction in the heat anomaly at the smectic-A_2–smectic-A_{2b} transition as X decreases can be explained assuming that the energy fluctuations around this transition are very sensitive to the ordering of the smectic-A_2 background.

ACKNOWLEDGMENTS

We are grateful to D. Miyajima and Professor T. Aida for synthesizing additional pure BO11 samples. This research was supported by the Global Center of Excellence Program by MEXT, Japan through the Nanoscience and Quantum Physics Project of the Tokyo Institute of Technology. This work was partly supported by the G-COE program (Education and Research Center for Material Innovation) at the Tokyo Institute of Technology. B.K.S. thanks the Indian National Science Academy, New Delhi for financial support.

[1] R. Pratibha, N. V. Madhusudana, and B. K. Sadashiva, Science **288**, 2184 (2000).
[2] R. Pratibha, N. V. Madhusudana, and B. K. Sadashiva, Phys. Rev. E **71**, 011701 (2005).
[3] Y. Takanishi, G. J. Shin, J. C. Jung, Suk-W. Choi, K. Ishikawa, J. Watanabe, H. Takezoe, and P. Toledano, J. Mater. Chem. **15**, 4020 (2005).
[4] M. E. Fisher, Phys. Rev. **176**, 257 (1968); M. E. Fisher and P. E. Scesney, Phys. Rev. A **2**, 825 (1970).
[5] T. A. Alvesalo, P. M. Berglund, S. T. Islander, G. R. Pickett, and W. Zimmermann, Phys. Rev. A **4**, 2354 (1971).
[6] D. A. Huse, Phys. Rev. Lett. **55**, 2228 (1985).
[7] M. E. Huster, K. J. Stine, and C. W. Garland, Phys. Rev. A **36**, 2364 (1987).
[8] J. Caerels, C. Glorieux, and J. Thoen, Phys. Rev. E **65**, 031704 (2002).
[9] M. A. Anisimov, A. V. Voronel, and T. M. Ovodova, Sov. Phys. JETP **34**, 583 (1972).
[10] M. A. Anisimov, A. V. Voronel, and E. E. Gorodetski, Sov. Phys. JETP **33**, 605 (1971).
[11] W. L. McMillan, Phys. Rev. A **4**, 1238 (1971).
[12] See, for instance, S. Chandrasekhar, *Liquid Crystals* (Cambridge University Press, Cambridge, England, 1992).
[13] W. L. McMillan, Phys. Rev. A **6**, 936 (1972).
[14] C. W. Garland and G. Nounesis, Phys. Rev. E **49**, 2964 (1994).
[15] H. Marynissen, J. Thoen, and W. Van Dael, Mol. Cryst. Liq. Cryst. **124**, 195 (1985).
[16] M. B. Sied, J. Salud, D. O. López, M. Barrio, and J. Ll Tamarit, Phys. Chem. Chem. Phys. **4**, 2587 (2002).
[17] J. Thoen, H. Beringhs, J. M. Auguste, G. Sigaud, and G. Seynhaeve, Mol. Cryst. Liq. Cryst. **2**, 853 (1987).
[18] K. Ema and H. Yao, Thermochim. Acta **304/305**, 157 (1997).
[19] H. Yao, K. Ema, and C. W. Garland, Rev. Sci. Instrum. **69**, 172 (1998).
[20] F. J. Wegner, Phys. Rev. B **5**, 4529 (1972).
[21] M. Barmatz, P. C. Hohenberg, and A. Kornblit, Phys. Rev. B **12**, 1947 (1975).
[22] C. Bagnuls and C. Bervillier, Phys. Rev. B **32**, 7209 (1985).
[23] J. A. Potton and P. C. Lanchester, Phase Trans. **6**, 43 (1985).
[24] A. Aharony and G. Ahlers, Phys. Rev. Lett. **44**, 782 (1980).
[25] X. Wen, C. W. Garland, and G. Heppke, Phys. Rev. A **44**, 5064 (1991).
[26] C. Bervillier, Phys. Rev. B **34**, 8141 (1986).
[27] C. Bagnuls, C. Bervillier, D. I. Meiron, and B. G. Nickel, Phys. Rev. B **35**, 3585 (1987).
[28] D. Stauffer, M. Ferer, and M. Wortis, Phys. Rev. Lett. **29**, 345 (1972).
[29] P. C. Hohenberg, A. Aharony, B. I. Halperin, and E. D. Siggia, Phys. Rev. B **13**, 2986 (1976).
[30] D. Brisbin, R. DeHoff, T. E. Lockhart, and D. L. Johnson, Phys. Rev. Lett. **43**, 1171 (1979).
[31] C. W. Garland, G. B. Kasting, and K. J. Lushington, Phys. Rev. Lett. **43**, 1420 (1979).
[32] K. J. Lushington, G. B. Kasting, and C. W. Garland, Phys. Rev. B **22**, 2569 (1980).
[33] G. B. Kasting, K. J. Lushington, and C. W. Garland, Phys. Rev. B **22**, 321 (1980).